Report

Cell Reports

The Kinesin KIF21B Regulates Microtubule Dynamics and Is Essential for Neuronal Morphology, Synapse Function, and Learning and Memory

Graphical Abstract

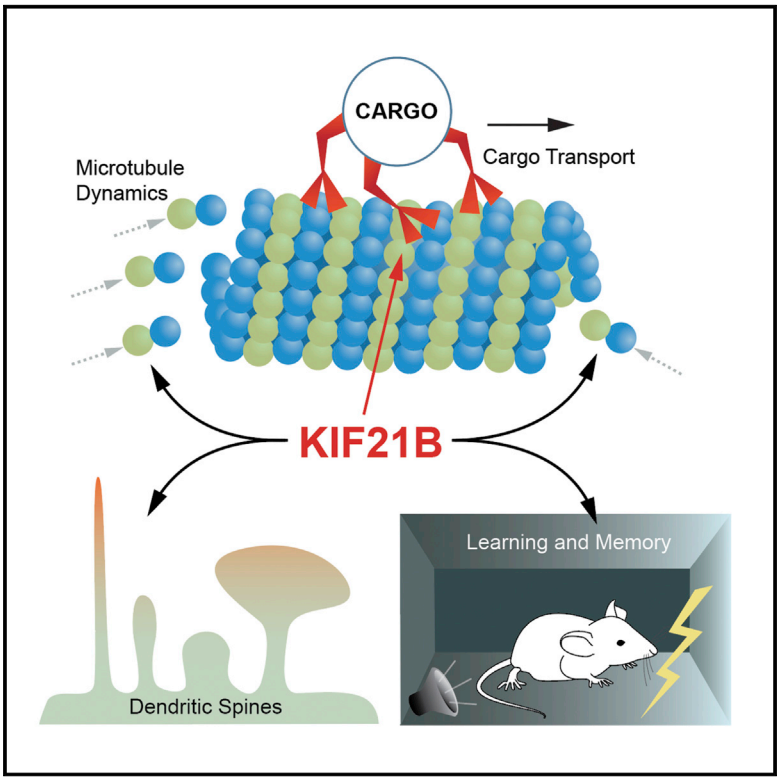

Authors

Mary Muhia, Edda Thies, Dorthe Labonté, ..., Jürgen R. Schwarz, Erika L.F. Holzbaur, Matthias Kneussel

Correspondence

matthias.kneussel@zmnh.uni-hamburg.de

In Brief

Muhia et al. investigate the physiological functions of the kinesin-4 member KIF21B. They show that KIF21B is a processive motor protein regulating microtubule dynamics. They also demonstrate that KIF21B depletion alters neuronal morphology by decreasing dendritic branching and spine number. In addition, *Kif21b* knockout mice are impaired in learning and memory.

Highlights

- KIF21B is a processive kinesin that regulates microtubule dynamics
- KIF21B depletion alters neuronal dendritic tree branching and spine formation
- *Kif21b* knockout mice exhibit learning and memory deficits

Muhia et al., 2016, Cell Reports *15*, 968–977
May 3, 2016
http://dx.doi.org/10.1016/j.celrep.2016.03.086

OPEN ACCESS
CellPress

Cell Reports
Report

The Kinesin KIF21B Regulates Microtubule Dynamics and Is Essential for Neuronal Morphology, Synapse Function, and Learning and Memory

Mary Muhia,[1,6] Edda Thies,[1,6] Dorthe Labonté,[1] Amy E. Ghiretti,[5] Kira V. Gromova,[1] Francesca Xompero,[2] Corinna Lappe-Siefke,[1] Irm Hermans-Borgmeyer,[3] Dietmar Kuhl,[2] Michaela Schweizer,[4] Ora Ohana,[2] Jürgen R. Schwarz,[1] Erika L.F. Holzbaur,[5] and Matthias Kneussel[1,*]

[1]Department of Molecular Neurogenetics
[2]Department of Molecular and Cellular Cognition
[3]Transgenic Animal Unit
[4]Morphology Unit, Center for Molecular Neurobiology ZMNH
University Medical Center Hamburg-Eppendorf, Falkenried 94, 20251 Hamburg, Germany
[5]Department of Physiology, University of Pennsylvania School of Medicine, Philadelphia, PA 19104-6085, USA
[6]Co-first author
*Correspondence: matthias.kneussel@zmnh.uni-hamburg.de
http://dx.doi.org/10.1016/j.celrep.2016.03.086

SUMMARY

The kinesin KIF21B is implicated in several human neurological disorders, including delayed cognitive development, yet it remains unclear how KIF21B dysfunction may contribute to pathology. One limitation is that relatively little is known about KIF21B-mediated physiological functions. Here, we generated *Kif21b* knockout mice and used cellular assays to investigate the relevance of KIF21B in neuronal and in vivo function. We show that KIF21B is a processive motor protein and identify an additional role for KIF21B in regulating microtubule dynamics. In neurons lacking KIF21B, microtubules grow more slowly and persistently, leading to tighter packing in dendrites. KIF21B-deficient neurons exhibit decreased dendritic arbor complexity and reduced spine density, which correlate with deficits in synaptic transmission. Consistent with these observations, *Kif21b*-null mice exhibit behavioral changes involving learning and memory deficits. Our study provides insight into the cellular function of KIF21B and the basis for cognitive decline resulting from KIF21B dysregulation.

INTRODUCTION

Kinesin superfamily proteins (KIFs) share a common ATP-binding "motor" domain, fused to divergent tail domains that specify intracellular localization and function. Many kinesins utilize chemical energy derived from ATP hydrolysis to propel directional transport of various cargoes along the microtubule (MT) cytoskeleton (Hirokawa et al., 2009). Kinesins have also been shown to regulate MT dynamics. For example, kinesin-4 and -8 family members adopt dual roles as cargo translocators and regulators of MT dynamics (Drummond, 2011; Walczak et al., 2013). These findings highlight a kinesin-MT interplay in mediating intracellular cargo transport (Hirokawa et al., 2009).

MTs are composed of α- and β-tubulin and bind specific protein complexes at their plus and minus ends (Jiang and Akhmanova, 2011; Yau et al., 2014). The plus ends of cellular MTs can dynamically remodel through stochastic length fluctuations. These events, termed as dynamic instability, comprise periods of persistent MT growth interrupted by occasional rapid shrinkage: switching between these states of growth and shortening is termed catastrophe and rescue (Gardner et al., 2013).

Studies from several mouse mutant lines have unraveled essential roles for kinesins and other MT binding proteins in neuronal development, survival, and higher brain function. Further, abnormalities in kinesin function and the MT cytoskeleton are reflected in a wide spectrum of human diseases, including neurodegeneration and cognitive disability (Franker and Hoogenraad, 2013; Hirokawa and Tanaka, 2015).

Kinesin-4 family members KIF21A and KIF21B were previously described to share little identity with other KIFs beyond the conserved motor domain, suggesting that they may play unique roles in vivo (Marszalek et al., 1999). KIF21A is expressed ubiquitously, and displays robust processive activity in vitro (Cheng et al., 2014). KIF21A binds to KANK1 (*ANKRD15*, KN motif, and ankyrin repeat domains 1) and co-clusters with liprins and components of the MT attachment complex at the cellular cortex. It inhibits MT growth and engages in organizing MT arrays at the cell edge (van der Vaart et al., 2013).

By contrast, KIF21B protein expression is restricted to the brain, spleen, and testes (Marszalek et al., 1999). Within neurons, KIF21B is present in axons and dendrites, with particular enrichment in growth cones of developing neurons (Huang and Banker, 2012; Marszalek et al., 1999). KIF21B binds E3 ubiquitin ligase TRIM3 (tripartite motif protein 3) to regulate $GABA_A$ receptor surface delivery (Labonté et al., 2013, 2014). Micro-duplications in the chromosomal region 1q32.1, including the *Kif21b* gene, have been described in individuals with delayed motor and

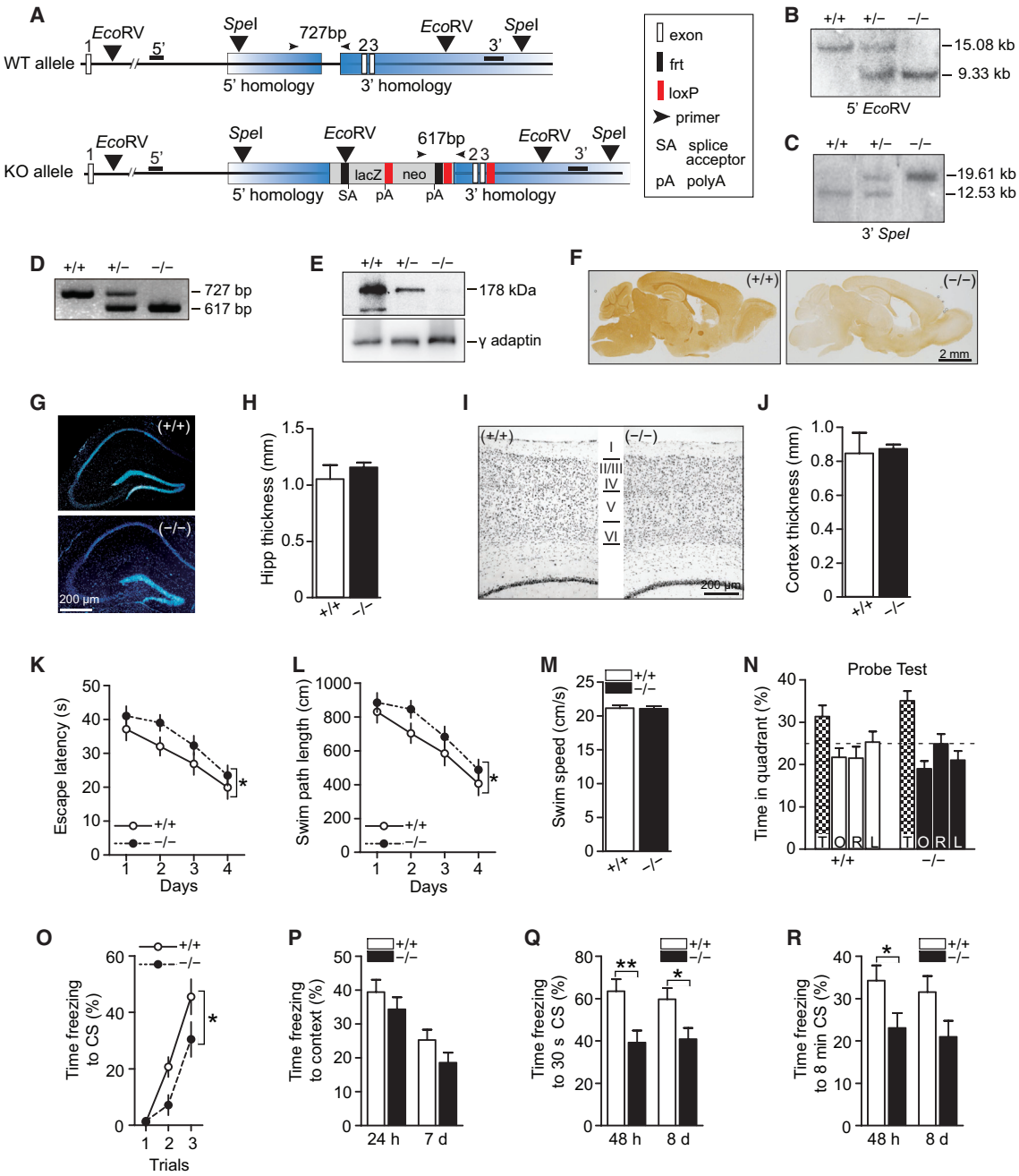

Figure 1. Targeting of the *Kif21b* Gene and Learning and Memory Deficits in *Kif21b*$^{-/-}$ Mice

(A) Scheme of targeting strategy. Southern restriction sites (*EcoRV* and *Spe*I: 5′ and 3′), location of respective probes, and PCR primer locations are indicated. KO alleles harbor three *LoxP* sites flanking the neo cassette and exons 2–3 of the *Kif21b* gene coding sequence. The targeting cassette is flanked by frt sites. Integration of the targeting vector results in a knockout-first allele.

(B and C) Southern blotting of genomic DNA performed using (B) 5′- and (C) 3′-flanking probes.

(D) PCR genotyping in $^{+/+}$, $^{+/-}$, and $^{-/-}$ mice.

(E) Western blot analysis probed with anti-KIF21B and anti-γ-adaptin (loading control).

(F) Immunohistochemical staining confirming loss of KIF21B immunoreactivity in $^{-/-}$ brain tissue.

(G and H) DAPI stain showing grossly normal hippocampal structure (G) and thickness (H) in $^{-/-}$ mice. p = 0.67.

(I and J) Nissl stain showing intact cortical lamination (I) and thickness (J; p = 0.91) in $^{-/-}$ mice. Student's t test. ($^{+/+}$), n = 4, ($^{-/-}$), n = 3.

(K–N) Morris water maze test. Acquisition, as indexed by escape latency (K) and path length (L) to goal platform differs between genotypes. (M) Comparable swim speed for both groups across training (genotype: p = 0.98). (N) Spatial bias for the training quadrant in the probe test (Genotype: p = 0.44). Values represent

(legend continued on next page)

cognitive development (Olson et al., 2012). Additionally, polymorphisms in the *Kif21b* gene have been identified as a susceptibility locus for multiple sclerosis (MS) (Goris et al., 2010; International Multiple Sclerosis Genetics Consortium (IMSGC), 2010). More recently, KIF21B enrichment was linked to accelerated neurodegeneration in MS and Alzheimer's disease (AD). Indeed, its expression was increased several-fold in MS and AD patients at different ages and disease severity (Kreft et al., 2014).

Despite this potential clinical relevance, it is currently unclear how KIF21B dysfunction contributes to neuropathology, largely because the physiological function of KIF21B is not yet understood. Thus, insight into KIF21B-mediated mechanisms is instrumental in elucidating its influence on neuronal health. To this end, we generated a *Kif21b* knockout mouse and employed cellular assays of KIF21B depletion and overexpression in order to investigate its functional significance in cytoskeletal transport, neuronal integrity, and behavior. We show that KIF21B is a processive kinesin motor that also regulates MT dynamics. We identify a neuronal role for KIF21B in dendritic tree branching and spine formation and show that KIF21B is necessary for learning and memory. Overall, our studies characterize the function of KIF21B in neurons and provide insight into its role in cognition.

RESULTS

Generation and Verification of *Kif21b* Knockout Mice

To investigate the in vivo relevance of KIF21B, we generated *Kif21b* knockout ($^{-/-}$) mice (Figure 1A) using knockout first embryonic stem (ES) cells obtained from the Knockout Mouse Project repository (KOMP, clone no. 24702). Successful gene targeting was confirmed using Southern blotting and PCR analysis (Figures 1B–1D). Western blot experiments using a KIF21B-specific antibody (Figures S1A and S1B) confirmed loss of KIF21B in $^{-/-}$ mice (Figure 1E). Relative to $^{+/+}$ controls, immunohistochemical staining revealed the absence of detectable KIF21B signal above background levels in $^{-/-}$ brain tissue (Figures 1F and S1C). Thus, the targeting approach was effective in constitutively abolishing *Kif21b* gene expression in $^{-/-}$ mice without changing KIF21A expression levels (Figures S1D and S1E). This allowed us to investigate the influence of KIF21B on neuronal development, network integrity, and subsequent impact on adult behavior. *Kif21b*$^{-/-}$ mice were viable and showed no overt abnormalities (Figures S1F and S1G). Examination of Nissl-stained $^{-/-}$ brain sections revealed normal hippocampal structure (Figures 1G and 1H), and intact cortical lamination indistinguishable from $^{+/+}$ controls (Figures 1I and 1J). Further evaluation in young and aged *Kif21b* $^{+/+}$ and $^{-/-}$ brains revealed no discernable changes in astrogliosis (not shown) or neurodegeneration (Figure S1H).

Kif21b$^{-/-}$ Mice Exhibit Learning and Memory Deficits

While kinesins KIF17 and KIF1A have been implicated in learning and memory (Kondo et al., 2012; Wong et al., 2002; Yin et al., 2011), the involvement of other KIFs in cognition remains largely unexplored. On this basis, we sought to address the impact of *Kif21b* ablation on learning and memory processes. Assessment in a novel open-field arena revealed intact locomotor activity and habituation in $^{-/-}$ mice (Figure S1I). However, in the Morris water maze reference memory test, $^{-/-}$ mice displayed inferior spatial acquisition relative to $^{+/+}$ controls. Despite improving across training, $^{-/-}$ mice showed significantly longer latencies and distance to reach the goal platform (Figures 1K–1M). This impairment was limited to acquisition since both genotype groups demonstrated a focused preference for the target quadrant in the absence of the platform (Figure 1N). Hence, KIF21B depletion may interfere with the initial encoding of spatial information but may not be critical for spatial memory retrieval or retention.

To investigate whether this learning deficit translated to other cognitive domains, we tested the mice for cued conditioned fear memory. *Kif21b*$^{-/-}$ mice displayed comparatively weaker freezing responses to the tone conditioned stimulus (CS) during acquisition (Figure 1O). Upon re-exposure to the training context, both genotype groups exhibited comparable freezing levels (Figure 1P), suggesting that memory of background contextual cues is unaltered in $^{-/-}$ mice. We then examined the freezing response elicited by the CS by focusing on the first 30 s, when the length of the tone corresponds to that used during acquisition. Here, $^{-/-}$ mice showed significantly less freezing compared with $^{+/+}$ controls (Figure 1Q). Furthermore, the freezing response to the entire 8-min tone (extinction) was significantly decreased in $^{-/-}$ mice (Figure 1R). Thus, acquisition and memory of the tone CS was impaired in $^{-/-}$ mice. Together, these data indicate that KIF21B is critical for learning and memory function.

KIF21B Depletion Alters Neuronal Dendritic Tree Branching and Spine Formation

Adaptive changes in the structural and functional properties of neurons and neuronal networks are considered to represent the cellular basis for some forms of learning and memory (Bliss and Collingridge, 1993; Martin et al., 2000). Cognitive disturbances in *Kif21b*$^{-/-}$ mice may therefore stem from abnormalities in cellular and network morphology, or synaptic transmission. To this end, we examined long-term potentiation (LTP) and long-term depression (LTD) at hippocampal Schaffer collateral synapses. Theta burst stimulation (TBS) induced strong and long-lasting LTP in slices derived from $^{+/+}$ and $^{-/-}$ mice (Figure S2A). Similarly, a low-frequency stimulation protocol induced stable LTD in both genotype groups (Figure S2B). We then examined LTP using high-frequency stimulation (HFS), which evoked a long-lasting LTP in both $^{+/+}$ and $^{-/-}$ slices. However, we

mean ± SEM (*$p < 0.05$, acquisition: repeated-measures (RM) ANOVA; probe test: two-way ANOVA; swim speed: Student's t test). ($^{+/+}$) mice: n = 13 (males = 6, females = 7); ($^{-/-}$) mice: n = 17 (males = 9, females = 8). T, target; O, opposite; R, right; L, left quadrants.

(O–R) Cued fear conditioning test. (O) Acquisition of conditioned freezing response to the tone CS across three CS-US (tone-shock) pairings. (P) Expression of conditioned freezing response to the background context at 24 hr and 7 days after acquisition. (Q) Expression of freezing response to the 30-s tone CS 48 hr and 8 days after acquisition. (R) Freezing response to the 8-min CS (extinction) 48 hr and 8 days after acquisition. Values represent mean ± SEM (*$p < 0.05$, **$p < 0.01$: RM ANOVA or two-way ANOVA with post hoc comparisons). ($^{+/+}$) mice: n = 15 (males = 8, females = 7); ($^{-/-}$) mice: n = 15 (males = 9, females = 6).

See also Figure S1.

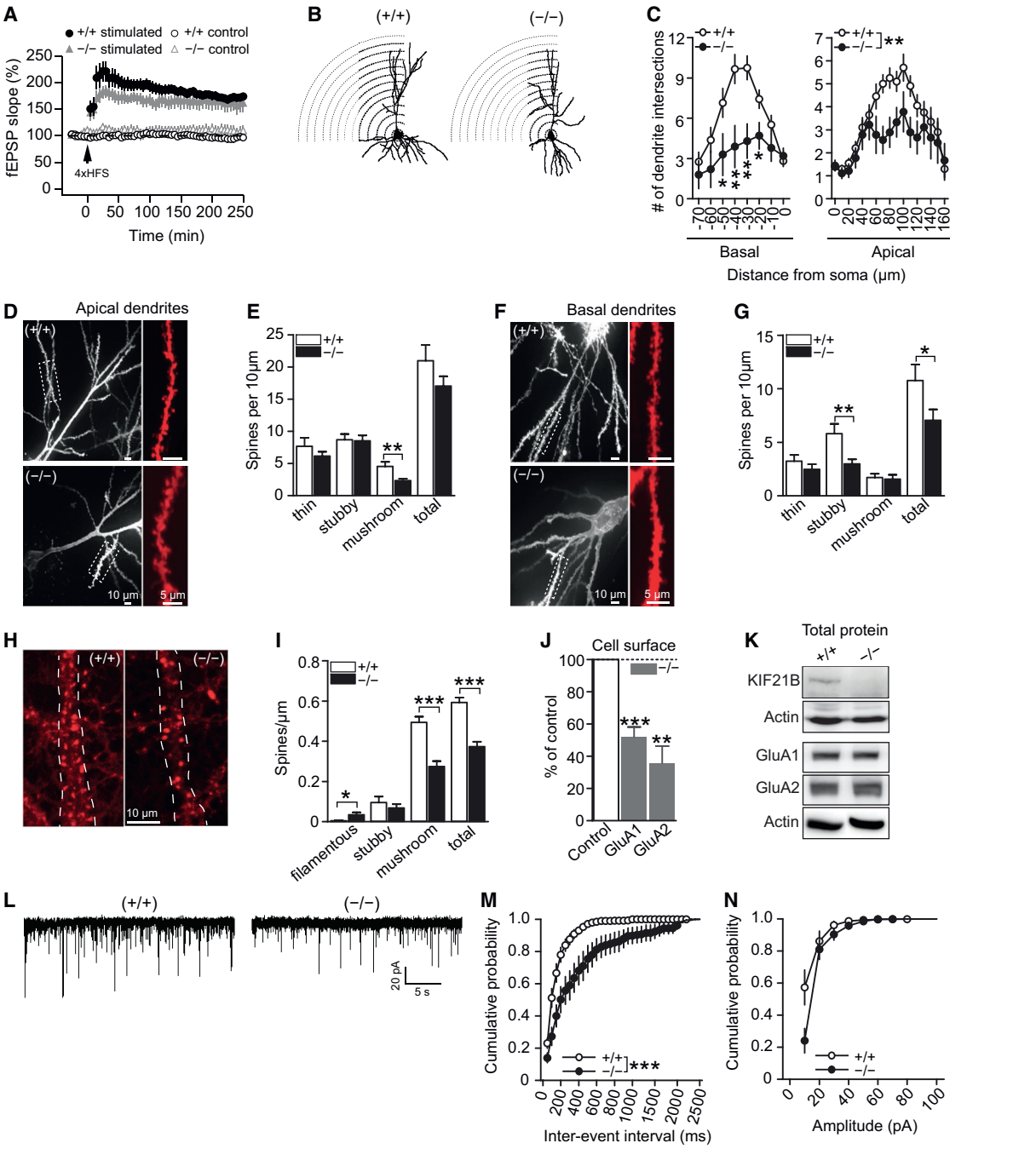

Figure 2. KIF21B Deficiency Alters Neuronal Morphology and Synaptic Function

(A) HFS-LTP (4×, arrow) at Schaffer collateral synapses. ANOVA, ($^{+/+}$), n = 12; ($^{-/-}$), n = 12.

(B and C) Diolistic (DiI) dye labeling and imaging in hippocampal slices. (B) Traces of reconstructed dendritic arbors. (C) Sholl analysis of dendrite intersections. RM ANOVA and post hoc comparisons. ($^{+/+}$), n = 10 neurons; ($^{-/-}$), n = 14 neurons.

(D–G) Spines from DiI-labeled CA1 pyramidal cell apical (D) and basal (F) dendrites. Insets, right: enlargements of boxed areas. (E and G) Spine type and density per 10 μm dendrite length. Student's t test. Apical branches: ($^{+/+}$), n = 8 neurons; ($^{-/-}$), n = 17 neurons; Basal branches: ($^{+/+}$), n = 10 neurons; ($^{-/-}$), n = 16 neurons.

(H and I) Spine analysis conducted in DIV22 neuronal cultures. (H) Representative images of neurons labeled with Phalloidin rhodamine. (I) Spine density per unit length of dendrite. Student's t test. ($^{+/+}$), n = 4 neurons, 15 dendrites; ($^{-/-}$), n = 7 neurons, 15 dendrites. Values expressed as mean ± SEM.

(J) Surface biotinylation assay on hippocampal slices. One sample t test against 100% loading control. n = 5–10 experiments.

(legend continued on next page)

observed a moderate attenuation in early-LTP from $^{-/-}$ slices ($p = 0.08$), suggestive of possible changes in induction of plasticity (Figures 2A and S2C).

We examined neuronal morphology by first assessing dendritic arbors from DiI-labeled CA1 pyramidal cells. Sholl analysis of reconstructed neurons (Figure 2B) revealed altered dendritic tree complexity in $^{-/-}$ neurons, corresponding to significantly less branching in both basal and apical dendrites (Figure 2C). Furthermore, the density of mushroom-type spines on apical dendrites (Figures 2D and 2E), and stubby-type and total spines on basal branches, was significantly decreased in $^{-/-}$ neurons (Figures 2F and 2G). Ultrastructural examination revealed intact postsynaptic densities (PSDs) in *Kif21b*$^{-/-}$ spines (Figures S2D and S2E), indicating that the morphology of existing spines remains unaltered.

We observed similar changes in spine density in cultured hippocampal *Kif21b*$^{-/-}$ neurons (Figures 2H and 2I), and in cultured $^{+/+}$ neurons following acute KIF21B short hairpin RNA (shRNA) knockdown (Figure S2F). In contrast to observations on KIF21B, we found that acute KIF21A knockdown did not alter spine density in $^{+/+}$ neurons nor exacerbate the spine phenotype in *Kif21b*$^{-/-}$ neurons (Figure S2G). Thus, the observed decrease in spine density is specific to KIF21B.

Since reductions in spine density might alter synapse function, we performed cell-surface biotinylation experiments to assess for possible changes in the levels of synaptic membrane proteins. The cell-surface levels of AMPA receptor (AMPAR), $GABA_A$ receptor ($GABA_AR$) subunits, and a neuroligin (Figures 2J and S2H), but not their total protein content (Figures 2K and S2I), were reduced in *Kif21b*$^{-/-}$ slices, suggesting a general reduction in synapse numbers. Accordingly, analysis of AMPAR-mediated spontaneous excitatory postsynaptic currents (EPSCs) revealed prolonged inter-event intervals in $^{-/-}$ neurons (Figures 2L–2M and S2J). However, the mEPSC amplitudes and mean current densities remained unchanged (Figures 2N and S2K) indicating that remaining synapses are functional. These observations were specific, since action potential properties were similar for both groups (Figures S2L–S2N), confirming that neurons were in a healthy condition. Together, these findings indicate that KIF21B is essential for the development of dendritic arbors, synapse number, and corresponding cell-surface expression of individual synaptic proteins.

KIF21B Displays Processive Activity

KIFs play a major role in neuronal function via their ability to propel cargo along the MT cytoskeleton (Hirokawa et al., 2009). To gain mechanistic insight into the sub-cellular role of KIF21B, we first examined its kinetic properties by employing an in vitro single-molecule motility assay. We characterized KIF21B motor activity using a Halo-tagged truncated form of the kinesin (KIF21B (1–657)), which lacks C-terminal residues that may be involved in autoinhibition. The movement of Halo-tagged KIF21B (1–657) could be visualized along Taxol-stabilized GFP-labeled MTs (average MT length: 45.6 μm). We found KIF21B to be processive, with run lengths of nearly 10 μm (average velocity = 0.43 μm/s; average run length = 8.8 μm). KIF21B particles remained on the MT for an average of 26.5 s before completing their runs and falling off (Figures 3A, left, 3B, and 3C). To exclude the possibility that the observed mobility may stem from hitchhiking on alternative motors, we introduced a point mutation in the motor domain KIF21B (1–657) T96N. The presence of the T96N mutation completely abolished particle mobility compared with the control fusion protein (KIF21B (1–657); Figure 3A, right), indicating that KIF21B moves processively independent of other drivers. In $^{+/+}$ neurons, we used a similar construct (mCherry-KIF21B (1–620)), which also revealed frequent mobile particles. Particles moved bi-directionally interspersed with pauses, at an average velocity of 0.4 μm/s (Figures 3D and 3E). Thus, KIF21B displays processive activity both in vitro and in neurons.

KIF21B Regulates MT Dynamics

Kinesin-4 family motors, including KIF21A, have been shown to regulate MT dynamics (Bringmann et al., 2004; van der Vaart et al., 2013). Since KIF21B shares 61% identity with KIF21A (Marszalek et al., 1999), KIF21B might also act to regulate MT dynamics. To test this hypothesis, we used the MT-plus end binding protein EB3 to image the growth of MTs in HeLa cells expressing full-length KIF21B, KIF21B (1–620), or KIF21B (T96N) fluorescent fusion proteins (Figure 3F). Overexpressed full-length KIF21B significantly increased MT growth rates (Figures 3G and 3H), whereas all fusion proteins, independent of the C-terminal truncation or the functional mutation in the motor domain, decreased the growth of +TIP-labeled MTs (Figures 3I and S3A). Thus, it appears that KIF21B motility may not be necessary for its ability to regulate MT growth.

We further employed total internal reflection fluorescence (TIRF) imaging and examined mRFP-α-tubulin-labeled MTs in HeLa cells. Full-length KIF21B, but not GFP-KIF21B (1–620), decreased the average MT lifetime prior to catastrophe (Figures 3J and S3B), independent of changes in tubulin posttranslational modifications (Figure S3C).

Next, we performed EB3 imaging in neurons and observed that +TIP-labeled MTs in KIF21B-deficient neurons had significantly slower growth rates. At the same time, the distance of MT growth was substantially longer in $^{-/-}$ neurons, compared with $^{+/+}$ neurons (Figures 4A–4D). Further ultrastructural examination revealed significantly shorter distances and tighter packing between adjacent MTs in *Kif21b*$^{-/-}$ dendrites (Figures 4E and 4F). Together these data indicate that, in addition to its role as a cargo motor, KIF21B acts by limiting MT growth and influences MT polymerization/de-polymerization rates.

Since MTs serve as cytoskeletal rails for active motor transport, changes in MT dynamics might, in turn, impact alternative kinesin-driven transport parameters. Therefore, we analyzed mitochondria motility, which is driven by kinesins 1 and 3

(K) Total protein content analysis using hippocampi from $^{+/+}$ and $^{-/-}$ mice. n = 3 experiments.
(L–N) Whole-cell patch-clamp recordings in 22 DIV neurons. (L) Sample current traces of mEPSCs. Cumulative probability histograms for mEPSC inter-event intervals (M) and amplitudes (N). KS test. ($^{+/+}$), n = 9; ($^{-/-}$), n = 11.
All graphs: *$p < 0.05$, **$p < 0.01$, ***$p < 0.001$. See also Figure S2.

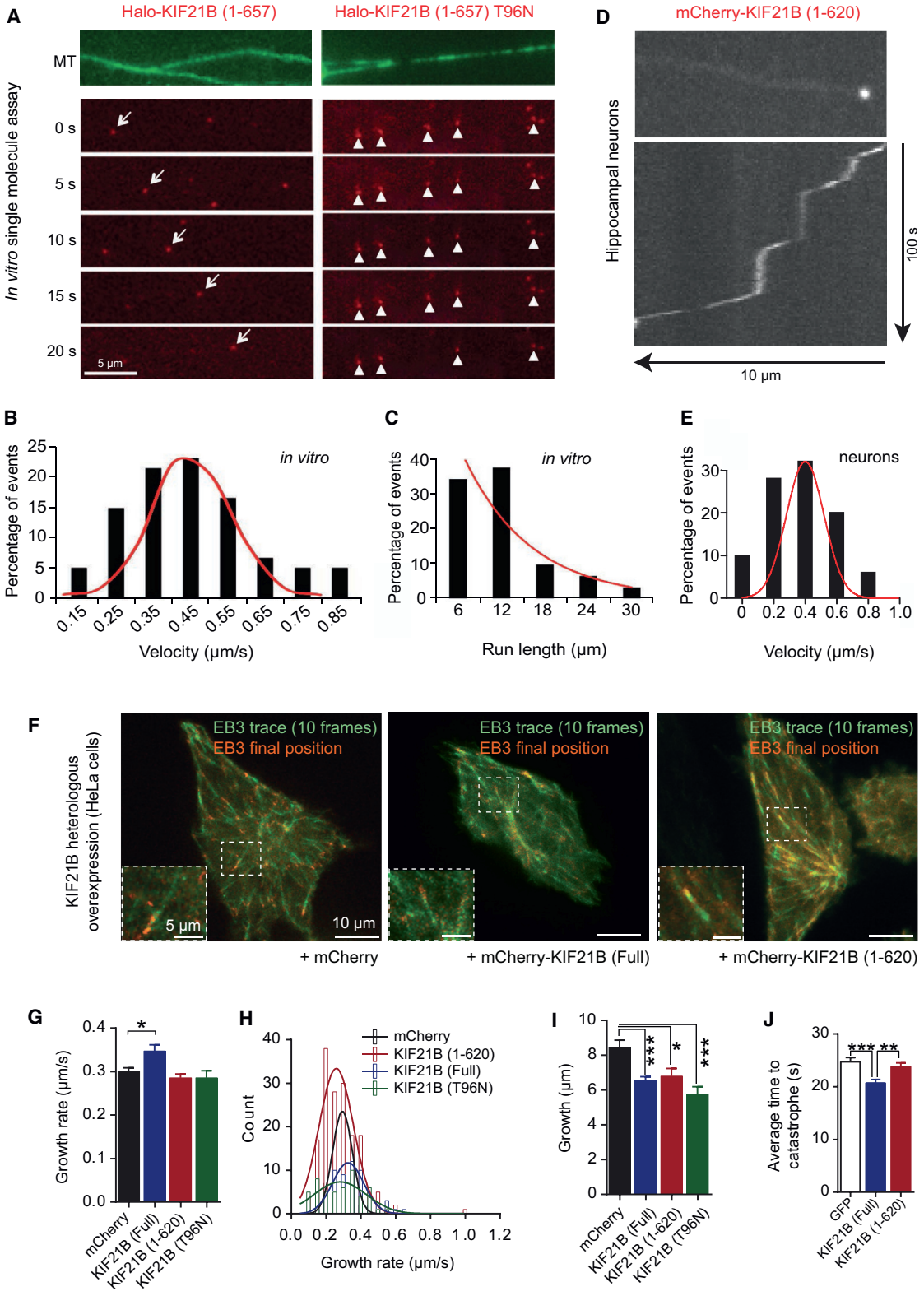

(legend on next page)

(Hirokawa et al., 2009; Lin and Sheng, 2015). Using Mito Tracker imaging, we observed that, whereas mitochondria traveled at similar speeds in *Kif21b*$^{+/+}$ and $^{-/-}$ neurons, the duration of movement was substantially reduced in $^{-/-}$ neurons, indicating that mitochondria travel over shorter distances (Figures 4G–4I). Additionally, we observed significantly less stationary mitochondria in $^{-/-}$ neurons (Figure 4J), suggesting that alterations of MT dynamics in KIF21B-depleted neurons might induce secondary changes on MT-based transport.

KIF21B Regulation of MT Dynamics Influences Spine Formation

A central role for MTs in spine formation and morphology is inferred from studies showing that activity-induced changes in MT dynamics lead to transient MT invasion of spines (Gu et al., 2008; Hu et al., 2008; Jaworski et al., 2009). Therefore, we explored the possibility that the observed defects in MT dynamics might contribute to the *Kif21b*$^{-/-}$ neuronal spine phenotype (Figures 2H and 2I). We re-expressed either full-length KIF21B or KIF21B (1–620) to assess their efficacy in normalizing spine number in *Kif21b*$^{-/-}$ neurons. Neurons were analyzed after 48 hr to avoid toxicity associated with protein overexpression over extended periods. Despite the modest time window, re-expression of either fusion protein significantly increased the number of filamentous spines. Moreover, full-length KIF21B and KIF21B (1–620) induced a partial but significant normalization of the total number of spines above KIF21B knockout background (Figures 4K and S3D). Re-expression of the C-terminal truncated KIF21B (1–620) fragment, which lacks the cargo-binding domain, was sufficient to mediate this effect. These results indicate that KIF21B's regulation of MT dynamics play an important role in spine formation, although it is likely that its role in cargo trafficking may also be involved.

DISCUSSION

The present study aimed to elucidate KIF21B-mediated mechanisms and functional significance in neurons and in vivo. We show that KIF21B is highly processive and, together with its known function in MT-dependent transport (Labonté et al., 2014), also identify a role for KIF21B in regulating MT dynamics. Thus, similar to other kinesin-4 family members (Drummond, 2011; Walczak et al., 2013), KIF21B exerts dual functions as a processive motor and MT regulator. However, it differs from KIF21A with respect to MT growth rates (van der Vaart et al., 2013). Unlike KIF21B, acute knockdown of KIF21A gene expression does not alter dendritic spine number (Figure S2G). Therefore, it seems unlikely that the two kinesins are functionally redundant. It is noteworthy that polymorphisms of either motor are implicated in distinct human neurological disorders.

We also identify an integral role for KIF21B in learning and memory, thereby providing further insight into the role of KIFs and their unique cargoes in modulating cognitive function (Kondo et al., 2012; Yin et al., 2011). *Kif21b*$^{-/-}$ mice were selectively impaired in spatial acquisition but displayed normal spatial memory, which is concomitant with largely intact hippocampal synaptic plasticity. One possibility is that KIF21B deficiency impedes learning by weakening the ability to form associations between spatial cues and the platform location. This view is reflected by the more severe deficits that emerged in associative fear learning. Hence, the relative contribution of KIF21B to memory appears to depend on the nature of the cognitive task (spatial versus emotional), and possibly the impact of KIF21B deficiency on extra-hippocampal substrates that underlie different forms of learning.

In evaluating network and neural correlates of the cognitive phenotype, we found that KIF21B depletion alters neuronal morphology and function by decreasing dendritic tree branching. Existing branches harbored fewer spines, which was accompanied by diminished neuronal mEPSC frequencies. However, it appears that synaptic receptor content in available spines may be sufficient to mediate adult network plasticity and correspond to unaltered mEPSC amplitudes in $^{-/-}$ neurons.

The observed neuronal abnormalities may stem from the developmental influence of KIF21B on neurite outgrowth. Indeed, KIF21B is enriched at growth cones located at neurite tips (Labonté et al., 2013), suggesting that its direct impact on MT dynamics is expected to influence neurite development and synaptogenesis. Dendrite morphogenesis and spine formation undergo dynamic structural remodeling prior to establishment of the network in adulthood (Koleske, 2013). These processes are intimately connected during development and are critically dependent on factors that influence MT dynamics and transport (Coles and Bradke, 2015; Conde and Cáceres, 2009). In this regard, there is increasing evidence linking MT dynamics to synaptic function and memory formation. For instance, growing MT plus ends decorated by the +TIP EB3 enter dendritic spines and can modulate spine morphology

Figure 3. KIF21B Is a Processive Motor and Regulates MT Dynamics

(A–C) In vitro motility assay of single KIF21B particles along MTs. (A) Motility of KIF21B (1-657; left panel) and of KIF21B (1–657) T96N, encoding a point mutation in the motor domain (right panel). The frequency distribution of velocity (B) and run lengths (C) of motile KIF21B particles are shown. Curves represent Gaussian and exponential decay fits, respectively. n = 93 particles.

(D and E) Time-lapse imaging conducted in neurons transfected with mCherry-KIF21B (1–620). (D) Kymograph illustrating dendritic movement of KIF21B particles. (E) Gaussian distribution and curve fit for particle velocity. n = 23 particles.

(F–I) Time-lapse imaging of +TIP EB3 dynamics. (F) HeLa cells expressing EB3 together with indicated constructs. Ten consecutive frames were averaged (trace: green). One image was superimposed (final position: red). Insets: enlargements of boxed areas. (G) Average growth rates of EB3 comets in HeLa cells expressing the corresponding constructs. (H) Frequency distribution of comet growth rates. Curves represent Gaussian fits. (I) Average EB3 comet growth in HeLa cells expressing the respective constructs. EB3/mCherry: seven cells, 69 comets, EB3/mCherry-KIF21B (1–620): eight cells, 55 comets, EB3/mCherry-KIF21B (full length): 17 cells, 167 comets, EB3/Halo-KIF21B (1–657) T96N: eight cells, 51 comets.

(J) TIRF-based live-cell imaging of mRFP-α-tubulin-labeled MTs in HeLa cells expressing the indicated GFP-fusion proteins. The graph depicts average MT lifetime prior to catastrophe. GFP control: 19 cells, 198 MTs, KIF21B (full length): 19 cells, 225 MTs, KIF21B (1–620): 20 cells, 224 MTs.

For averaged values (mean ± SEM), *$p < 0.05$, **$p < 0.01$, ***$p < 0.01$: one-way ANOVA followed by post hoc comparisons. See also Figure S3.

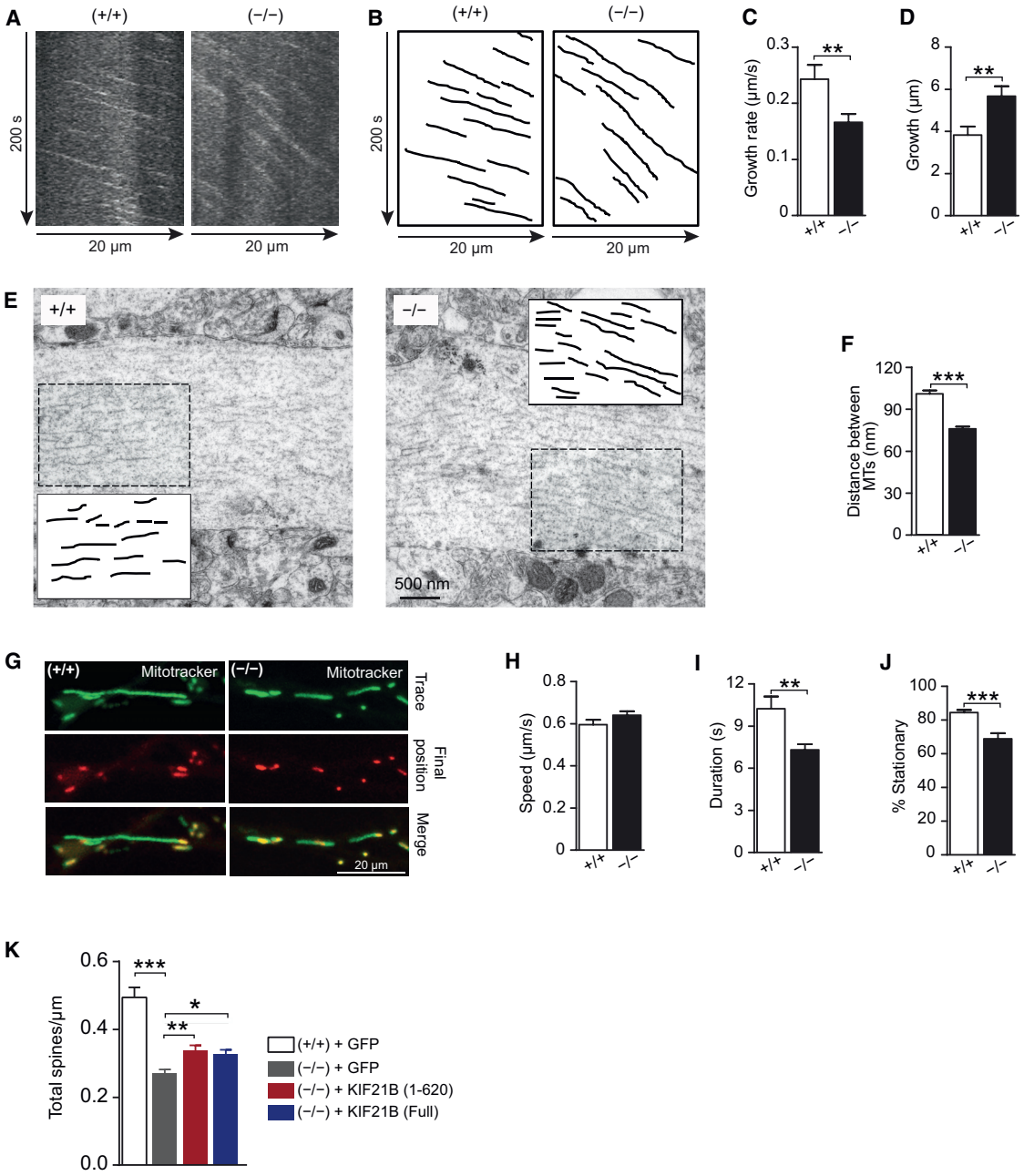

Figure 4. KIF21B Depletion Affects MT Dynamics

(A–D) Neuronal live-cell imaging and assessment of +TIP EB3-GFP-labeled MT dynamics. Kymographs (A) and corresponding traces (B) of EB3-GFP comets illustrating movement (displacement on the x axis) over time (y axis). MTs from $^{-/-}$ neurons grow significantly slower (C) but over longer distances (D). ($^{+/+}$), n = 41; ($^{-/-}$), n = 50 comets.

(E and F) Electron micrographs in which MTs were traced (inset rectangles) from dendrites of similar size and orientation. (F) Quantification and analysis of distance between adjacent microtubule traces. ($^{+/+}$), n = 21; ($^{-/-}$), n = 15 dendrites.

(G–J) Neuronal MitoTracker live imaging. (G) 30 consecutive frames (1 s/frame) were averaged (green trace), and the final position was superimposed (red). Graphs depict mitochondria speed (H), duration of movement (I), and number of stationary particles (J). ($^{+/+}$), n = 98; ($^{-/-}$), n = 141 particles.

(K) Quantification of spine number per micrometer dendrite in hippocampal neurons at 10 DIV transfected with KIF21B (full length) and KIF21B (1–620) fusion proteins. Ten to 12 neurons per transfected construct. ($^{+/+}$) + GFP, 18 dendrites; ($^{-/-}$) + GFP, 23 dendrites; ($^{-/-}$) + KIF21B (1–620), 57 dendrites; ($^{-/-}$) + KIF21B (full length), 47 dendrites.

All values represent mean ± SEM, *p < 0.05, **p < 0.01, ***p < 0.001: Student's t test and one-way ANOVA followed by post hoc comparisons. See also Figure S3.

(Jaworski et al., 2009). Diminished MT turnover and stability are associated with reduced spine density and impaired memory formation (Fanara et al., 2010).

Given that MTs serve as cytoskeletal rails for active motor transport, alterations in MT dynamics are anticipated to induce secondary changes on MT-based transport. Thus, it is not surprising that depletion of a MT dynamics regulator, such as KIF21B, affects mitochondria transport driven by alternative motors. Since the two mechanisms are not mutually exclusive (MT dynamics and transport), the phenotypes owing to *Kif21b* gene ablation are likely to stem from altered MT integrity and corresponding changes in MT-based transport parameters.

Impairments in MT dynamics and cytoskeletal transport are a hallmark feature in neurological disorders (Dubey et al., 2015; Franker and Hoogenraad, 2013). The identification of KIF21B in regulating MT dynamics and transport may represent a common mechanism in neurological disorders associated with KIF21B dysfunction. Subcellular consequences of a defective KIF21B-MT interplay may cause deleterious effects in central and peripheral neuronal subtypes that harbor long axons, and which critically depend on cytoskeletal transport. However, we cannot exclude a currently un-identified role for KIF21B in immune disorders because KIF21B is detected in the spleen and other cell types including oligodendrocytes (Dugas et al., 2006).

KIF21B levels are abnormally elevated in MS and AD (Kreft et al., 2014), including a mouse model for AD (Figures S3E and S3F). Thus, together with our findings on KIF21B depletion, it is apparent that the precise dose of KIF21B is necessary for neuronal function. Since the ratio of stable to dynamic microtubule populations is critical in neurons, complete depletion or chronic several-fold increase of KIF21B will topple this equilibrium, thereby disrupting neuronal integrity. In keeping with this, it would be of interest to examine whether such changes exist on the MT cytoskeleton in induced pluripotent stem (ips) cell-derived neurons from MS and AD patients. Altogether, our data represent an initial step to delineate the mechanisms involving KIF21B-mediated MT dynamics and trafficking in the context of cognitive function, and increased risk for the disorders in which this motor is implicated.

EXPERIMENTAL PROCEDURES

The generation of *Kif21b* knockout mice and in vivo experiments were conducted in accordance with the German and European Union laws on protection of experimental animals following approval by the local authorities of the City of Hamburg (Committee for Lebensmittelsicherheit und Veterinärwesen, Authority of Soziales, Familie, Gesundheit und Verbraucherschutz Hamburg, Germany, No. 90/10 and 100/13). Detailed descriptions of the materials and methods can be found in Supplemental Experimental Procedures.

Time-Lapse Imaging of Microtubule Dynamics and Mitochondria Motility

To examine MT dynamics, 10 days in vitro (DIV) neurons were transfected with EB3-GFP. For mitochondria analysis, 4 DIV neurons were labeled with 100 nM MitoTracker Red CMXRos (Life Technologies). Time-lapse imaging was performed using a Nikon spinning disc confocal microscope at 1 frame/s for 200 s and 1 frame/2 s, respectively. The speed and growth of EB3-GFP mobile comets and analysis of mitochondria movement were done with ImageJ (NIH).

In Vitro Single-Molecule Motility Assay

HeLa cells were transfected with either Halo-tagged KIF21B (1–657) or KIF21B (1–657) T96N. Motility assays with cell extracts were performed as described (Ayloo et al., 2014). Images were captured using a Nikon TIRF system (Perkin Elmer) on an inverted Ti microscope (five frames/s for 120 s). Subsequent analysis was done using the ImageJ TrackMate plugin.

TIRF Imaging of MTs

HeLa cells were transfected with mRFP-tubulin and GFP, GFP-KIF21B (full length), or GFP-KIF21B (1–620), respectively. Total internal reflection fluorescence (TIRF) microscopy was performed on a Nikon Spinning disc microscope equipped with a Nikon CFI Apo TIRF 100 × 1.49 DNA oil objective and the 561-nm laser to visualize MT at the vicinity of the cell cortex. Images were taken every 1 s for 300 frames. To assess the stability of MT, the average lifetime of single MTs before catastrophe was quantified. Quantification was done manually using Volocity (Improvision).

Whole-Cell Patch-Clamp Recordings

Recordings were conducted on dissociated hippocampal neurons (DIV 20–22) at 21°C–23°C. The Patchmaster software with the EPC-9 patch-clamp amplifier (HEKA) was used for stimulation and data acquisition. Recordings with an access resistance <20 MΩ were evaluated using Fitmaster (HEKA), Igor Pro 6.03 (Wavemetrics), Mini Analysis (Synaptosoft), and Excel (Microsoft).

Behavioral Analyses

Male and female mice were 10–12 weeks old at the time of testing in the water maze and conditioned freezing experiments.

SUPPLEMENTAL INFORMATION

Supplemental Information includes Supplemental Experimental Procedures and three figures and can be found with this article online at http://dx.doi.org/10.1016/j.celrep.2016.03.086.

AUTHOR CONTRIBUTIONS

D.L., I.H.-B., C.L.-S., and E.T. generated and verified the KO mouse. M.M. performed and analyzed the behavioral experiments. M.M. analyzed cell biological and electrophysiological data and performed the statistical analysis. E.T. performed and analyzed the neuronal and synaptic morphology data, biochemical western-blot-based assays, neuronal motility assays, and MT dynamics assays. A.E.G. and E.L.F.H. performed and analyzed the in vitro single-molecule motility assay. K.V.G. performed and analyzed the TIRF imaging of MTs. J.R.S. performed and analyzed the whole-cell patch-clamp recordings. F.X., O.O., and D.K. performed and analyzed the in vitro field recordings. M.S. performed the electron microscopy analysis. M.K. designed the study, analyzed data, and wrote the manuscript with the help of M.M. and E.T.

ACKNOWLEDGMENTS

We thank S. Hoffmeister-Ullerich for help with genomic PCR, A. Akhmanova for EB3-GFP, R. Tsien for mRFP-α-tubulin, and Eva-Maria Mandelkow and A. Sydow for TG4510 mice. This work is supported by Deutsche Forschungsgemeinschaft (DFG) grants FOR 2419, project KN556/11-1 and GRK1459 project KN556/14592 and the Hamburg Landesforschungsförderung (LFF) to M.K.

Received: August 25, 2015
Revised: February 19, 2016
Accepted: March 24, 2016
Published: April 21, 2016

REFERENCES

Ayloo, S., Lazarus, J.E., Dodda, A., Tokito, M., Ostap, E.M., and Holzbaur, E.L. (2014). Dynactin functions as both a dynamic tether and brake during dynein-driven motility. Nat. Commun. *5*, 4807.

Bliss, T.V., and Collingridge, G.L. (1993). A synaptic model of memory: long-term potentiation in the hippocampus. Nature *361*, 31–39.

Bringmann, H., Skiniotis, G., Spilker, A., Kandels-Lewis, S., Vernos, I., and Surrey, T. (2004). A kinesin-like motor inhibits microtubule dynamic instability. Science *303*, 1519–1522.

Cheng, L., Desai, J., Miranda, C.J., Duncan, J.S., Qiu, W., Nugent, A.A., Kolpak, A.L., Wu, C.C., Drokhlyansky, E., Delisle, M.M., et al. (2014). Human CFEOM1 mutations attenuate KIF21A autoinhibition and cause oculomotor axon stalling. Neuron *82*, 334–349.

Coles, C.H., and Bradke, F. (2015). Coordinating neuronal actin-microtubule dynamics. Curr. Biol. *25*, R677–R691.

Conde, C., and Cáceres, A. (2009). Microtubule assembly, organization and dynamics in axons and dendrites. Nat. Rev. Neurosci. *10*, 319–332.

Drummond, D.R. (2011). Regulation of microtubule dynamics by kinesins. Semin. Cell Dev. Biol. *22*, 927–934.

Dubey, J., Ratnakaran, N., and Koushika, S.P. (2015). Neurodegeneration and microtubule dynamics: death by a thousand cuts. Front. Cell. Neurosci. *9*, 343.

Dugas, J.C., Tai, Y.C., Speed, T.P., Ngai, J., and Barres, B.A. (2006). Functional genomic analysis of oligodendrocyte differentiation. J. Neurosci. *26*, 10967–10983.

Fanara, P., Husted, K.H., Selle, K., Wong, P.Y., Banerjee, J., Brandt, R., and Hellerstein, M.K. (2010). Changes in microtubule turnover accompany synaptic plasticity and memory formation in response to contextual fear conditioning in mice. Neuroscience *168*, 167–178.

Franker, M.A., and Hoogenraad, C.C. (2013). Microtubule-based transport - basic mechanisms, traffic rules and role in neurological pathogenesis. J. Cell Sci. *126*, 2319–2329.

Gardner, M.K., Zanic, M., and Howard, J. (2013). Microtubule catastrophe and rescue. Curr. Opin. Cell Biol. *25*, 14–22.

Goris, A., Boonen, S., D'hooghe, M.B., and Dubois, B. (2010). Replication of KIF21B as a susceptibility locus for multiple sclerosis. J. Med. Genet. *47*, 775–776.

Gu, J., Firestein, B.L., and Zheng, J.Q. (2008). Microtubules in dendritic spine development. J Neurosci. *28*, 12120–12124.

Hirokawa, N., and Tanaka, Y. (2015). Kinesin superfamily proteins (KIFs): various functions and their relevance for important phenomena in life and diseases. Exp. Cell Res. *334*, 16–25.

Hirokawa, N., Noda, Y., Tanaka, Y., and Niwa, S. (2009). Kinesin superfamily motor proteins and intracellular transport. Nat. Rev. Mol. Cell Biol. *10*, 682–696.

Hu, X., Viesselmann, C., Nam, S., Merriam, E., and Dent, E.W. (2008). Activity-dependent dynamic microtubule invasion of dendritic spines. J Neurosci. *28*, 13094–13105.

Huang, C.F., and Banker, G. (2012). The translocation selectivity of the kinesins that mediate neuronal organelle transport. Traffic *13*, 549–564.

International Multiple Sclerosis Genetics Consortium (IMSGC) (2010). Comprehensive follow-up of the first genome-wide association study of multiple sclerosis identifies KIF21B and TMEM39A as susceptibility loci. Hum. Mol. Genet. *19*, 953–962.

Jaworski, J., Kapitein, L.C., Gouveia, S.M., Dortland, B.R., Wulf, P.S., Grigoriev, I., Camera, P., Spangler, S.A., Di Stefano, P., Demmers, J., et al. (2009). Dynamic microtubules regulate dendritic spine morphology and synaptic plasticity. Neuron *61*, 85–100.

Jiang, K., and Akhmanova, A. (2011). Microtubule tip-interacting proteins: a view from both ends. Curr. Opin. Cell Biol. *23*, 94–101.

Koleske, A.J. (2013). Molecular mechanisms of dendrite stability. Nat. Rev. Neurosci. *14*, 536–550.

Kondo, M., Takei, Y., and Hirokawa, N. (2012). Motor protein KIF1A is essential for hippocampal synaptogenesis and learning enhancement in an enriched environment. Neuron *73*, 743–757.

Kreft, K.L., van Meurs, M., Wierenga-Wolf, A.F., Melief, M.J., van Strien, M.E., Hol, E.M., Oostra, B.A., Laman, J.D., and Hintzen, R.Q. (2014). Abundant kif21b is associated with accelerated progression in neurodegenerative diseases. Acta Neuropathol. Commun. *2*, 144.

Labonté, D., Thies, E., Pechmann, Y., Groffen, A.J., Verhage, M., Smit, A.B., van Kesteren, R.E., and Kneussel, M. (2013). TRIM3 regulates the motility of the kinesin motor protein KIF21B. PLoS ONE *8*, e75603.

Labonté, D., Thies, E., and Kneussel, M. (2014). The kinesin KIF21B participates in the cell surface delivery of γ2 subunit-containing GABAA receptors. Eur. J. Cell Biol. *93*, 338–346.

Lin, M.Y., and Sheng, Z.H. (2015). Regulation of mitochondrial transport in neurons. Exp. Cell Res. *334*, 35–44.

Marszalek, J.R., Weiner, J.A., Farlow, S.J., Chun, J., and Goldstein, L.S. (1999). Novel dendritic kinesin sorting identified by different process targeting of two related kinesins: KIF21A and KIF21B. J. Cell Biol. *145*, 469–479.

Martin, S.J., Grimwood, P.D., and Morris, R.G. (2000). Synaptic plasticity and memory: an evaluation of the hypothesis. Annu. Rev. Neurosci. *23*, 649–711.

Olson, H.E., Shen, Y., Poduri, A., Gorman, M.P., Dies, K.A., Robbins, M., Hundley, R., Wu, B., and Sahin, M. (2012). Micro-duplications of 1q32.1 associated with neurodevelopmental delay. Eur. J. Med. Genet. *55*, 145–150.

van der Vaart, B., van Riel, W.E., Doodhi, H., Kevenaar, J.T., Katrukha, E.A., Gumy, L., Bouchet, B.P., Grigoriev, I., Spangler, S.A., Yu, K.L., et al. (2013). CFEOM1-associated kinesin KIF21A is a cortical microtubule growth inhibitor. Dev. Cell *27*, 145–160.

Walczak, C.E., Gayek, S., and Ohi, R. (2013). Microtubule-depolymerizing kinesins. Annu. Rev. Cell Dev. Biol. *29*, 417–441.

Wong, R.W., Setou, M., Teng, J., Takei, Y., and Hirokawa, N. (2002). Overexpression of motor protein KIF17 enhances spatial and working memory in transgenic mice. Proc. Natl. Acad. Sci. USA *99*, 14500–14505.

Yau, K.W., van Beuningen, S.F., Cunha-Ferreira, I., Cloin, B.M., van Battum, E.Y., Will, L., Schätzle, P., Tas, R.P., van Krugten, J., Katrukha, E.A., et al. (2014). Microtubule minus-end binding protein CAMSAP2 controls axon specification and dendrite development. Neuron *82*, 1058–1073.

Yin, X., Takei, Y., Kido, M.A., and Hirokawa, N. (2011). Molecular motor KIF17 is fundamental for memory and learning via differential support of synaptic NR2A/2B levels. Neuron *70*, 310–325.